NANO: Brief Reports and Reviews
Vol. 9, No. 5 (2014) 1440001 (7 pages)
© World Scientific Publishing Company
DOI: 10.1142/S1793292014400013

World Scientific
www.worldscientific.com

HIGH-EFFICIENT SOLID-STATE PEROVSKITE SOLAR CELL WITHOUT LITHIUM SALT IN THE HOLE TRANSPORT MATERIAL

DONGQIN BI*, GERRIT BOSCHLOO* and ANDERS HAGFELDT*,†,‡
*Department of Chemistry-Ångström Laboratory
Uppsala University, Box 532
SE 751 20 Uppsala, Sweden

†School of Chemical Engineering
Sungkyunkwan University, Suwon 440-746, Korea
‡anders.hagfeldt@kemi.uu.se

Received 24 February 2014
Accepted 25 March 2014
Published 5 June 2014

NANO Downloaded from www.worldscientific.com
by NANYANG TECHNOLOGICAL UNIVERSITY on 06/10/14. For personal use only.

CH_3NH_3PbX (X=Br, I, Cl) perovskites have recently been used as light absorbers in hybrid organic–inorganic solid-state solar cells, with efficiencies above 15%. To date, it is essential to add Lithium bis(Trifluoromethanesulfonyl)Imide (LiTFSI) to the hole transport materials (HTM) to get a higher conductivity. However, the detrimental effect of high LiTFSI concentration on the charge transport, DOS in the conduction band of the TiO_2 substrate and device stability results in an overall compromise for a satisfactory device. Using a higher mobility hole conductor to avoid lithium salt is an interesting alternative. Herein, we successfully made an efficient perovskite solar cell by applying a hole conductor PTAA (Poly[bis(4-phenyl) (2,4,6-trimethylphenyl)-amine]) in the absence of LiTFSI. Under AM 1.5 illumination of 100 mW/cm^2, an efficiency of 10.9% was achieved, which is comparable to the efficiency of 12.3% with the addition of 1.3 mM LiTFSI. An unsealed device without Li^+ shows interestingly a promising stability.

Keywords: Perovskite $CH_3NH_3PbI_3$; solar cell; lithium.

1. Introduction

Compared to traditional resources such as coal and fossil fuels, solar energy is a sustainable alternative to meet the rising energy demand and reduce the global warming. Making good use of this vast energy source requires a new generation of photovoltaics that are both efficient and cost-effective.[1] Novel approaches include dye-sensitized solar cells,[2,3] organic solar cells and inorganic–organic hybrid hetero-junction solar cells using inorganic nanocrystalline semiconductors and quantum dots.[4,5] Recently, CH_3NH_3PbX (X=Br, I, Cl) perovskites were introduced as light harvesters in solar cells. Since the first reports,[6,7] the solid state perovskite solar cell has been developed very fast to reach a power conversion efficiency (PCE) above 15%.[8,9] Several studies have reported on solar cell structure,[7,10–12] alternative organic materials,[13–15] charge transport mechanism,[16–18] perovskite preparing methods,[8,19,20] flexible solar cell,[21–23] and modules.[24] Although perovskite solar cell can also work without hole transport material (HTM), with a PCE

NANO Downloaded from www.worldscientific.com
by NANYANG TECHNOLOGICAL UNIVERSITY on 06/10/14. For personal use only.

of 5–8%,[12,25] transient absorption results show that the most efficient charge separation is obtained when using TiO_2 and HTM together. This is rationalized by the fact that the recombination process will be slower if the photogenerated electrons and holes are separated in the TiO_2 and HTM phases, respectively.[16] Many hole transporters have been tried, for example, poly(3-hexylthiophene-2,5-diyl) (P3HT),[26,27] 4-(diethylamino)-benzaldehyde diphenylhydrazone (DEH),[26] (Poly[bis(4-phenyl) (2,4,6-trimethylphenyl)amine]) PTAA,[27,28] poly-[2,1,3-benzothiadiazole-4,7-diyl[4,4-bis(2-ethylhexyl)-4H-cyclopenta[2,1-b:3,4-b′]dithiophene-2,6-diyl]] (PCPDTBT),[27] (poly-[[9-(1-octylnonyl)-9H-carbazole-2,7-diyl]-2,5-thiophenediyl-2,1,3-benzothiadiazole-4,7-diyl-2,5-thiophenediyl]) (PCDTBT),[27] poly [N-9-hepta-decanyl-2,7-carbazole-alt-3,6-bis-(thiophen-5-yl)-2,5-dioctyl-2,5-di-hydropyrrolo[3,4-]pyrrole-1,4-dione] (PCBTDPP),[29] pyrene arylamine derivatives[30] and CuI.[31] Up to now, spiro-OMeTAD is still the most efficient one for the solid-state perovskite solar cells as well as the solid-state dye-sensitized solar cells (ssDSCs). From a practical view point, however, there are still some obstacles during the fabrication process. More fundamentally, an issue is the low hole mobility. The conductivity of the pristine spiro-OMeTAD exhibits 2.0×10^{-4} Scm^{-1},[32] which is about 10-fold lower than that with p-type doping. Therefore, several kinds of dopants have been developed for spiro-OMeTAD, such as $(p\text{-}BrC_6H_4)_3NSbCl_6$,[3] tris(2-(1H-pyrazol-1-yl)pyridine) cobalt(III),[33] $SnCl_4$,[34] $SbCl_5$[35] and $FeCl_3$,[36] WO_3,[37] molybdenum tris[1,2-bis(trifluoromethyl)ethane-1, 2-dithiolene][38] and F4-TCNQ.[39] However, many of them are usually applied by vacuum deposition or have a poor solubility in organic solvent.[33] Lithium bis(Trifluoromethanesulfonyl)Imide (LiTFSI) has been found to be a crucial additive for spiro-OMeTAD to get an increment of conductivity,[40] a better electron injection[41] and retarded recombination.[42] However, the doping with LiTFSI is highly dependent on O_2,[43] and the lithium ions may be consumed during the doping process, which can affect the device performance and stability.[42] Herein, we have succeeded to make an efficient device without LiTFSI. We first optimize the PTAA solar cell with different addition of LiTFSI. The results showed that the solar cell performance is comparable with and without LiTFSI, but interestingly, the device without Li^+ shows a better stability.

2. Results and Discussion

The perovskite solar cells investigated here have the general structure FTO/TiO_2-blocking layer/mesoporous-TiO_2, perovskite and HTM/Au. A two-step deposition method was used for coating the mesoporous TiO_2 film with perovskite.[8] To investigate the effect of LiTFSI on the performance of PTAA and Spiro-OMeTAD solar cell, we kept a constant concentration of TBP (200 mM for Spiro-OMeTAD, 50 mM for PTAA). For different concentrations of LiTFSI to fabricate PTAA and spiro-OMeTAD solar cells, the photovoltaic parameters are shown in Fig. 1. For the PTAA solar cell, with the increase of LiTFSI from 0 mM to 1.3 mM, the average J_{sc} increases from 18.3 mA/cm^2 to 19.6 mA/cm^2, FF from 0.61 to 0.64 and PCE from 10.7% to 11.9%. The V_{oc} gradually decreases from 0.96 V to 0.89 V when the LiTFSI concentration increases from 0 mM to 20 mM. For spiro-OMeTAD, with the increase of LiTFSI from 20 mM to 60 mM, the average J_{sc} increased from 12.9 mA/cm^2 to 20 mA/cm^2, while FF increased from 0.5 to 0.69, simultaneously the V_{oc} increased from 0.88 to 0.98 and the PCE from 5.7% to 13.9%. It is noticeable that LiTFSI has a small effect on the PTAA solar cell, while it is important for the spiro-OMeTAD solar cell. The *J–V* curve and incident photon to current conversion efficiency (IPCE) spectra of the champion solar cell of PTAA and spiro-OMeTAD are shown in Fig. 2. By adding 1.3 mM LiTFSI, we achieve a 12.3% high-efficiency solar cell, with a J_{sc} of 20 mA/cm^2, V_{oc} of 0.94 V and FF of 0.66. By adding 60 mM LiTFSI, the spiro-OMeTAD shows a highest efficiency of 13.9% with a J_{sc} of 21.3 mA/cm^2, V_{oc} of 0.99 and FF of 0.66. Although spiro-OMeTAD shows a better performance, PTAA shows a good performance (10.9%) even when LiTFSI is absent.

As seen above, the most significant parameter that varies between spiro-OMeTAD and PTAA and Li^+ concentration is the short-circuit photocurrent. For PTAA, it remains high and constant, independent of the Li^+ concentration besides a small increase from 0 to 0.5 mM Li^+. This we attribute to a downward shift of the TiO_2 conduction band leading to an improved injection process of photoexcited electrons in the perovskite to the conduction band of TiO_2. For spiro-OMeTAD, the J_{sc} is significantly increased with addition of Li^+. Interestingly, it goes through a maximum at about 10 mM Li^+. Such a

NANO Downloaded from www.worldscientific.com
by NANYANG TECHNOLOGICAL UNIVERSITY on 06/10/14. For personal use only.

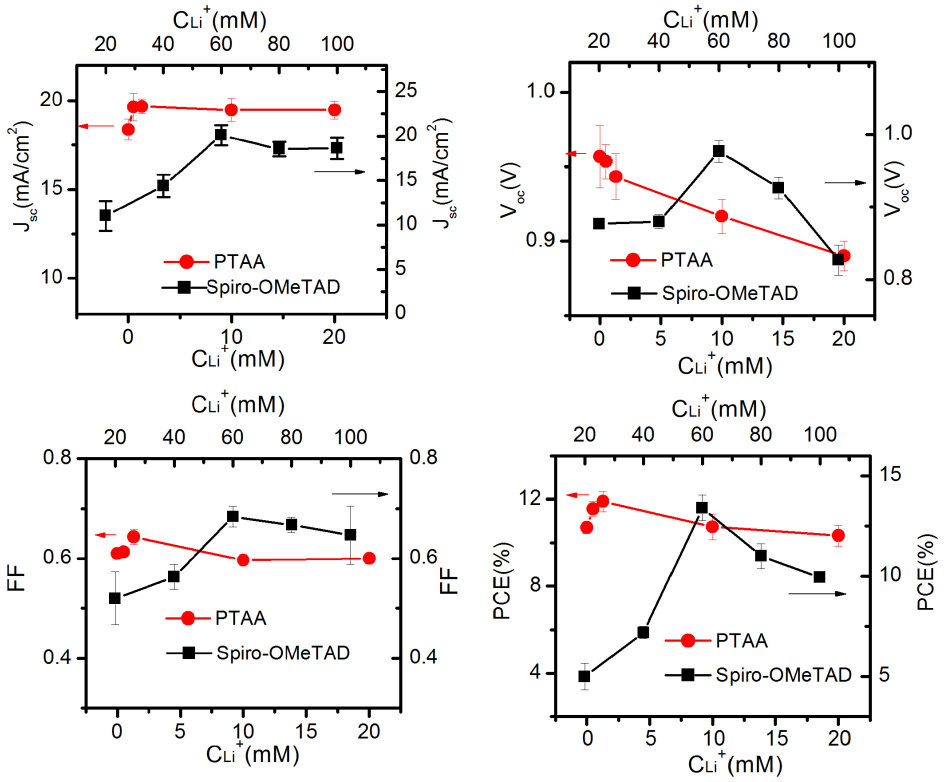

Fig. 1. Photovoltaic parameters of $TiO_2/CH_3NH_3PbI_3$/HTM/Au devices with different additions of LiTFSI, HTM: PTAA/Spiro-OMeTAD. (The left and the bottom axis are for PTAA, the top and right axis are for spiro-OMeTAD.)

variation of J_{sc} with Li^+ concentration in spiro-OMeTAD has been observed by Abate *et al.* for solid-state *dye-sensitized* solar cells.[42] This is a complex phenomenon and is discussed in the paper by Abate *et al.* in terms of improved electron injection from the excited dye to the TiO_2 conduction band, improved charge dynamics at the TiO_2-dye-spiro-OMeTAD interface, as well as effects on charge carrier transport in TiO_2 and spiro-OMeTAD. Interestingly, the authors in Ref. 42 conclude that an HTM with a substantially higher hole mobility, on the order of $10^{-3}\,cm^2\,V^{-1}s^{-1}$, than spiro-OMeTAD would be beneficial for further optimization of the efficiency of a solid-state dye-sensitized solar cell. The fact that the short circuit current in the present paper, replacing the dye-layer with the perovskite material, shows the same trend as in Ref. 42 indicates that the effect of Li^+ in spiro-OMeTAD is similar irrespective of using dyes or perovskite as light absorber. The high efficiency obtained in the

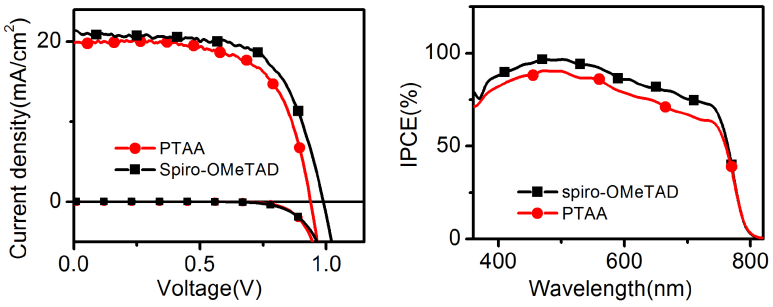

(a) (b)

Fig. 2. (a) *J–V* curve of $TiO_2/CH_3NH_3PbI_3$/HTM/Au devices under AM 1.5 illumination of 100 mw/cm^2 and in the dark (b) IPCE spectra of $TiO_2/CH_3NH_3PbI_3$/HTM/Au devices. HTM: PTAA/Spiro-OMeTAD.

NANO Downloaded from www.worldscientific.com
by NANYANG TECHNOLOGICAL UNIVERSITY on 06/10/14. For personal use only.

present work with PTAA as HTM with a hole mobility of 10^{-3}–10^{-2} cm^2 V^{-1} s^{-1},[44] confirms thus the prediction of Abate *et al.*, albeit our results are based on perovskite instead of dyes as light absorbing material. The main finding that J_{sc} is almost independent of Li^+ concentration for PTAA as HTM we attribute to the higher conductivity of this material making the solar cell device not limited by a series resistance of the hole transport.

To further compare our results with the work by Abate *et al.*, and in order to get insight into the reason for the different effects of LiTFSI on the two types of devices in the present paper, we measure the electron lifetime and the transient current decay.

2.1. *Electron lifetime measurements*

The electron lifetime was measured using a galvanostat at a constant current. A small square-wave modulation of the light intensity on top of a much larger bias light will result in small variations of the measured voltage, as the galvanostat keeps the current constant. On a downward step in light intensity, the electron concentration will decrease. The adjustment of electron concentration occurs by recombination only as the current and the bias light are fixed. The time constant found by measuring the voltage decay is therefore the electron lifetime. In Fig. 3, it is shown that, with the increase of Li^+, the electron lifetime increases for both the PTAA and spiro-OMeTAD devices. The reason that lifetime increases with Li^+ concentration can be attributed to "screening" of the Coulomb attraction between holes in the HTM and electrons in the TiO_2 by the high ion content as described by Abate *et al.*,[42] Contrasting the observation that V_{oc} decreases with Li^+ concentration with PTTA as HTM with the increase of electron lifetime in Fig. 3(b), the lowering of V_{oc} is reasonable to be explained by a downward shift of the TiO_2 conduction band. This also means that lithium ions are present at the TiO_2 surface even if there was a poor infiltration of PTAA in the mesopores of the TiO_2.[27]

2.2. *Transport time measurements*

The photocurrent response under potentiostatic conditions was used to determine electron transport times. The measured response time (t_{resp}) depends on both the electron transport time (t_{tr}) and the electron lifetime. The influence of the electron lifetime (t_e) can usually be neglected under short-circuit conditions. The following relation has been derived for the response time under potentiostatic conditions: $(t_{resp})^{-1} = (t_e)^{-1} + (t_{tr})^{-1}$. It has been shown that the transport time in mesostructured perovskite cells does not depend significantly on the hole mobility of the HTM, suggesting that the transport time in these measurements is limited by electron conduction.[45] Here, a slower transport time is observed with the increase of Li^+ concentration in both devices using spiro-OMeTAD or PTAA as HTM, respectively (Fig. 4). The reason may be, as discussed by Abate *et al.*,[42] that more Li^+ introduces a broader density of sub bandgap states. This will increase the average trap depth at any given charge density, electrons will be trapped in a deeper trap state, the time for the electron to be detrapped will be longer, resulting in a slower charge transport.

2.3. *Initial stability tests*

We measured the stability of the PTAA solar cell with and without LiTFSI. The unsealed solar cells are stored and measured in a humidity of 50–60%. In Fig. 5, we observe that the device with LiTFSI shows a relatively poorer stability, the V_{oc}, J_{sc} and

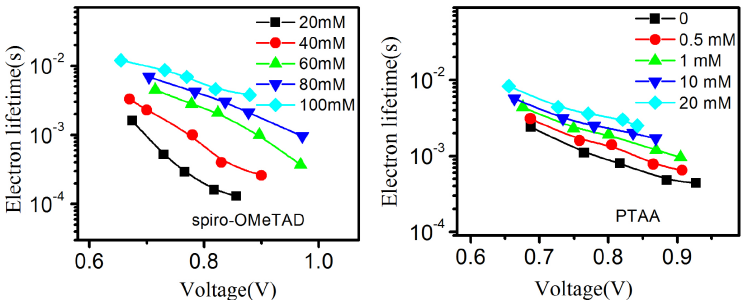

Fig. 3. Electron lifetime of $TiO_2/CH_3NH_3PbI_3$/HTM/Au devices. HTM: PTAA/Spiro-OMeTAD.

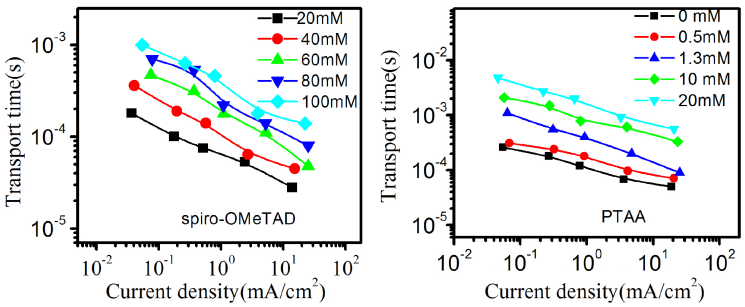

Fig. 4. Transient current decay of $TiO_2/CH_3NH_3PbI_3$/HTM/Au devices. HTM: PTAA/Spiro-OMeTAD.

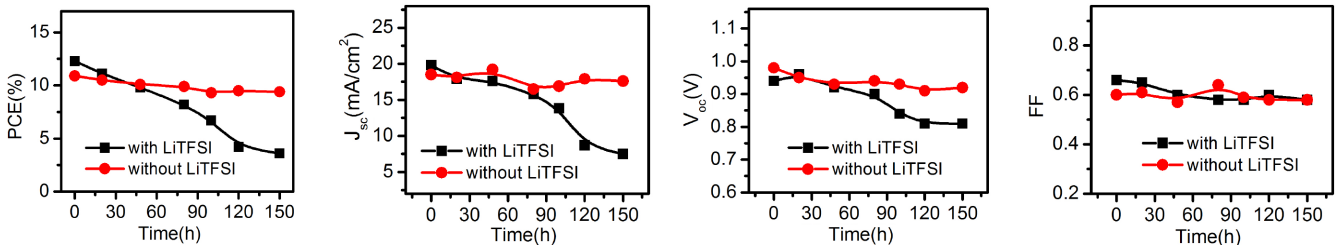

Fig. 5. Stability of $TiO_2/CH_3NH_3PbI_3$/PTAA/Au devices with and without LiTFSI (Relative humidity: 50–60%).

NANO Downloaded from www.worldscientific.com
by NANYANG TECHNOLOGICAL UNIVERSITY on 06/10/14. For personal use only.

FF keep decreasing with time. After 150 h, the PCE decreased from 12.3% to 3.6%, J_{sc} from 19.8 mA/cm^2 to 7.5 mA/cm^2, V_{oc} from 0.94 V to 0.81 V, FF from 0.66 to 0.58. However, for the device without Li^+, a better stability is observed, the PCE can still be 9.4% after 150 h. This can be due to several reasons; one possibility is that Li^+ is hygroscopic, and since the perovskite $CH_3NH_3PbI_3$ is also sensitive to water, a longer exposure of the device in moisture is detrimental to the device stability. These results indicate that it is possible to greatly improve the stability of the cells fabricated from perovskite without Li^+ salt in the HTMs.

3. Conclusion

An efficient perovskite solar cell was fabricated in the absence of LiTFSI, by applying a higher mobility hole conductor PTAA. Under AM 1.5 illumination of 100 mW/cm^2, an efficiency of 10.9% was achieved, which is comparable to the efficiency of 12.3% with the addition of 1.3 mM LiTFSI. Charge transport and recombination kinetics were also conducted. The results showed that LiTFSI can increase the electron lifetime and transport time in the two devices. It is also shown that the solar cell has a higher stability without LiTFSI of interest for further development of perovskite solar cells.

4. Methods

A 50 nm compact TiO_2 blocking layer was first deposited onto the surface of a pre-cleaned FTO substrate by spray pyrolysis on a hotplate at 500°C using 0.2 M Ti-isopropoxide, 2 M acetylaceton in isopropanol. For the nanostructured layer, TiO_2 was deposited by spin-coating the diluted Dyesol paste (18NR-T). A PbI_2 layer is deposited from 1 mol/L PbI_2 in Dimethylformamide solution with a spin-coating speed of 7000 rpm, $CH_3NH_3PbI_3$ was deposited by dipping the slide into a 10 mg/mL CH_3NH_3I in iso-propanol solution, as is described in Ref. 8. The coated films were then placed on a hot plate set at 100°C for 10 min in air. The composition of HTM was 0.170 M 2,2′, 7,7′-tetrakis-(N,N-di-p-methoxyphenyl-amine)-9,99-spirobifluorene (spiro-OMeTAD, Lumtec.), 15 mM PTAA, the additive of bis(trifluoromethane)sulfonimide lithium salt (LiTFSI, 99.95%, Aldrich) and 4-tert-butylpyridine (TBP, 99%, Aldrich) were added according to the text above. The $(CH_3NH_3)PbI_3$ sensitized TiO_2 films were coated with HTM solution using the spin-coating method at 4000 rpm. For the electrical contact, a 200 nm Au film was deposited onto the solar cell by thermal evaporation.

Current–voltage (J–V) characteristics were measured using a Keithley 2400 source/meter and a Newport solar simulator (model 91160) giving light

NANO Downloaded from www.worldscientific.com
by NANYANG TECHNOLOGICAL UNIVERSITY on 06/10/14. For personal use only.

with AM 1.5 G spectral distribution, which was calibrated using a certified reference solar cell (Fraunhofer ISE) to an intensity $1000\,W/m^2$. A black mask of $0.127\,cm^2$ was applied on top of the cell to avoid significant additional contribution from light falling on the device outside the active area. The *J–V* scan was made from V_{oc} to short J_{sc} with a time delay at V_{oc} of 20 s and a scan rate of 50 mV/s.

IPCE spectra were recorded using a computer-controlled setup consisting of a xenon light source (Spectral Products ASBXE-175), a monochromator (Spectral Products CM110) and a potentiostat (EG&G PAR 273), calibrated using a certified reference solar cell (Fraunhofer ISE).

Electron lifetime and transport times were performed using a white LED (Luxeon Star 1W) as the light source. Voltage and current traces were recorded with a 16-bit resolution digital acquisition board (National Instruments) in combination with a current amplifier (Stanford Research Systems SR570) and a custom-made system using electromagnetic switches. Transport time and lifetimes were determined by monitoring photocurrent and photovoltage transients at different light intensities upon applying a small square wave modulation to the base light intensity. The electron lifetime measured with transient photovoltage was calculated using the following equation: $V_{oc} = V_{oc,0} + \Delta V \exp(-t/\tau)$, where ΔV is the change in open-circuit voltage (V_{oc}) due to the modulated small change in light intensity, $V_{oc,0}$ is the open-circuit voltage before the change in light intensity and τ is the electron lifetime. The photocurrent and photovoltaic responses were fitted using first-order kinetics to obtain time constants.

Acknowledgments

We thank the Swedish Energy Agency, the Swedish Research Council (VR), the Göran Gustafsson Foundation and the Knut and Alice Wallenberg Foundation for financial support.

References

1. A. Hagfeldt, G. Boschloo, L. Sun, L. Kloo and H. Pettersson, *Chem. Rev.* **110**, 6595 (2010).
2. A. Yella, H. W. Lee, H. N. Tsao, C. Y. Yi and A. K. Chandiran, *Science* **334**, 1203 (2011).
3. U. Bach, D. Lupo, P. Comte, J. E. Moser, F. Weissortel, J. Salbeck, H. Spreitzer and M. Gratzel, *Nature* **395**, 583 (1998).
4. O. E. Semonin, J. M. Luther, S. Choi, H. Y. Chen, J. B. Gao, A. J. Nozik and M. C. Beard, *Science* **334**, 1530 (2011).
5. K. De Greve, L. Yu, P. L. McMahon, J. S. Pelc, C. M. Natarajan, N. Y. Kim, E. Abe, S. Maier, C. Schneider, M. Kamp, S. Hofling, R. H. Hadfield, A. Forchel, M. M. Fejer and Y. Yamamoto, *Nature* **491**, 421 (2012).
6. H. S. Kim, C. R. Lee, J. H. Im, K. B. Lee, T. Moehl, A. Marchioro, S. J. Moon, R. Humphry-Baker, J. H. Yum, J. E. Moser, M. Gratzel and N. G. Park, *Sci. Rep.* **2**, 591 (2012).
7. M. M. Lee, J. Teuscher, T. Miyasaka, T. N. Murakami and H. J. Snaith, *Science* **338**, 643 (2012).
8. J. Burschka, N. Pellet, S. J. Moon, R. Humphry-Baker, P. Gao, M. K. Nazeeruddin and M. Gratzel, *Nature* **499**, 316 (2013).
9. M. Z. Liu, M. B. Johnston and H. J. Snaith, *Nature* **501**, 395 (2013).
10. D. Q. Bi, G. Boschloo, S. Schwarzmuller, L. Yang, E. M. J. Johansson and A. Hagfeldt, *Nanoscale* **5**, 11686 (2013).
11. O. Malinkiewicz, A. Yella, Y. H. Lee, G. M. Espallargas, M. Gratzel, M. K. Nazeeruddin and H. J. Bolink, *Nat. Photonics* **8**, 128 (2014).
12. L. Etgar, P. Gao, Z. Xue, Q. Peng, A. K. Chandiran, B. Liu, M. K. Nazeeruddin and M. Grätzel, *J. Am. Chem. Soc.* **134**, 17396 (2012).
13. G. E. Eperon, S. D. Stranks, C. Menelaou, M. B. Johnston, L. M. Herz and H. J. Snaith, *Energ. Environ. Sci.* **7**, 982 (2014).
14. J. H. Im, J. Chung, S. J. Kim and N. G. Park, *Nanoscale Res. Lett.* **7**, 353 (2012).
15. S. Pang, H. Hu, J. Zhang, S. Lv, Y. Yu, F. Wei, T. Qin, H. Xu, Z. Liu and G. Cui, *Chem. Mater.* **26**, 1485 (2014).
16. A. Marchioro, J. Teuscher, D. Friedrich, M. Kunst, R. van de Krol, T. Moehl, M. Gratzel and J.-E. Moser, *Nat. Photonics* **8**, 250 (2014).
17. S. D. Stranks, G. E. Eperon, G. Grancini, C. Menelaou, M. J. P. Alcocer, T. Leijtens, L. M. Herz, A. Petrozza and H. J. Snaith, *Science* **342**, 341 (2013).
18. G. Xing, N. Mathews, S. Sun, S. S. Lim, Y. M. Lam, M. Grätzel, S. Mhaisalkar and T. C. Sum, *Science* **342**, 344 (2013).
19. D. Q. Bi, S. J. Moon, L. Haggman, G. Boschloo, L. Yang, E. M. J. Johansson, M. K. Nazeeruddin, M. Gratzel and A. Hagfeldt, *RSC Adv.* **3**, 18762 (2013).
20. Q. Chen, H. Zhou, Z. Hong, S. Luo, H.-S. Duan, H.-H. Wang, Y. Liu, G. Li and Y. Yang, *J. Am. Chem. Soc.* **136**, 622 (2013).

NANO Downloaded from www.worldscientific.com
by NANYANG TECHNOLOGICAL UNIVERSITY on 06/10/14. For personal use only.

21. J. You, Z. Hong, Y. Yang, Q. Chen, M. Cai, T.-B. Song, C.-C. Chen, S. Lu, Y. Liu and H. Zhou, *ACS Nano* **8**, 1674 (2014).
22. C. Roldan-Carmona, O. Malinkiewicz, A. Soriano, G. Minguez Espallargas, A. Garcia, P. Reinecke, T. Kroyer, M. I. Dar, M. K. Nazeeruddin and H. J. Bolink, *Energ. Environ. Sci.* **7**, 994 (2014).
23. P. Docampo, J. M. Ball, M. Darwich, G. E. Eperon and H. J. Snaith, *Nat. Commun.* **4**, 2761 (2013).
24. F. Matteocci, S. Razza, F. Di Giacomo, S. Casaluci, G. Mincuzzi, T. M. Brown, A. D'Epifanio, S. Licoccia and A. Di Carlo, *Phys. Chem. Chem. Phys.* **16**, 3918 (2014).
25. W. A. Laban and L. Etgar, *Energy Environ. Sci.* **6**, 3249 (2013).
26. D. Bi, L. Yang, G. Boschloo, A. Hagfeldt and E. M. J. Johansson, *J. Phys. Chem. Lett.* **4**, 1532 (2013).
27. J. H. Heo, S. H. Im, J. H. Noh, T. N. Mandal, C.-S. Lim, J. A. Chang, Y. H. Lee, H.-J. Kim, A. Sarkar, M. K. Nazeeruddin, M. Gratzel and S. I. Seok, *Nat. Photonics* **7**, 486 (2013).
28. J. H. Noh, S. H. Im, J. H. Heo, T. N. Mandal and S. I. Seok, *Nano Lett.* **13**, 1764 (2013).
29. B. Cai, Y. D. Xing, Z. Yang, W. H. Zhang and J. S. Qiu, *Energy Environ. Sci.* **6**, 1480 (2013).
30. N. J. Jeon, J. Lee, J. H. Noh, M. K. Nazeeruddin, M. Grätzel and S. I. Seok, *J. Am. Chem. Soc.* **135**, 19087 (2013).
31. J. A. Christians, R. C. M. Fung and P. V. Kamat, *J. Am. Chem. Soc.* **136**, 758 (2013).
32. D. Poplavskyy and J. Nelson, *J. Appl. Phys.* **93**, 341 (2003).
33. J. Burschka, A. Dualeh, F. Kessler, E. Baranoff, N. L. Cevey-Ha, C. Y. Yi, M. K. Nazeeruddin and M. Gratzel, *J. Am. Chem. Soc.* **133**, 18042 (2011).
34. M. Xu, Y. G. Rong, Z. L. Ku, A. Y. Mei, X. Li and H. W. Han, *J. Phys. Chem. C* **117**, 22492 (2013).
35. C. Ganzorig and M. Fujihira, *Appl. Phys. Lett.* **77**, 4211 (2000).
36. J. Endo, T. Matsumoto and J. Kido, *Jpn. J. Appl. Phys.* **41**, L358 (2002).
37. J. Meyer, S. Hamwi, S. Schmale, T. Winkler, H.-H. Johannes, T. Riedl and W. Kowalsky, *J. Mater. Chem.* **19**, 702 (2009).
38. Y. Qi, T. Sajoto, S. Barlow, E.-G. Kim, J.-L. Brédas, S. R. Marder and A. Kahn, *J. Am. Chem. Soc.* **131**, 12530 (2009).
39. D.-Y. Chen, W.-H. Tseng, S.-P. Liang, C.-I. Wu, C.-W. Hsu, Y. Chi, W.-Y. Hung and P.-T. Chou, *Phys. Chem. Chem. Phys.* **14**, 11689 (2012).
40. H. J. Snaith and M. Gratzel, *Appl. Phys. Lett.* **89**, 262114 (2006).
41. A. Furube, R. Katoh, K. Hara, T. Sato, S. Murata, H. Arakawa and M. Tachiya, *J. Phys. Chem. B* **109**, 16406 (2005).
42. A. Abate, T. Leijtens, S. Pathak, J. Teuscher, R. Avolio, M. E. Errico, J. Kirkpatrik, J. M. Ball, P. Docampo, I. McPherson and H. J. Snaith, *Phys. Chem. Chem. Phys.* **15**, 2572 (2013).
43. U. B. Cappel, T. Daeneke and U. Bach, *Nano Lett.* **12**, 4925 (2012).
44. W. Zhang, J. Smith, R. Hamilton, M. Heeney, J. Kirkpatrick, K. Song, S. E. Watkins, T. Anthopoulos and I. McCulloch, *J. Am. Chem. Soc.* **131**, 10814 (2009).
45. Y. Zhao, A. M. Nardes and K. Zhu, *J. Phys. Chem. Lett.* **5**, 490 (2014).